Chemical Engineering Journal 225 (2013) 120–127

Contents lists available at SciVerse ScienceDirect

Chemical Engineering Journal

journal homepage: www.elsevier.com/locate/cej

Process analysis on CO_2 absorption by monoethanolamine solutions in microchannel reactors

Chunbo Ye [a,b], Minhui Dang [a,b], Chaoqun Yao [a,b], Guangwen Chen [a,*], Quan Yuan [a]

[a] Dalian National Laboratory for Clean Energy, Dalian Institute of Chemical Physics, Chinese Academy of Sciences, Dalian 116023, China
[b] University of Chinese Academy of Sciences, Beijing 100049, China

HIGHLIGHTS

- Process of CO_2 absorption by MEA solutions was analyzed in microchannel reactors.
- Effects of relevant parameters on the process were evaluated.
- k_1 for CO_2 reaction with MEA was successfully determined under ambient pressure.
- An Arrhenius-type equation was obtained for k_1 for CO_2 absorption in microchannel.

ARTICLE INFO

Article history:
Received 6 January 2013
Received in revised form 9 March 2013
Accepted 12 March 2013
Available online 27 March 2013

Keywords:
CO_2 capture
Monoethanolamine
Reaction rate constant
Microreactor
FLNG

ABSTRACT

Process of CO_2 absorption by monoethanolamine (MEA) solutions was conducted in microchannel reactors and effects of several parameters on the absorption process were evaluated and analyzed, i.e., MEA concentration, temperature, pressure, molar ratio of MEA to CO_2 and aspect ratio of microchannel. Based on the process characteristics of CO_2 absorption in microchannel, a method was proposed to determine the reaction rate constant between CO_2 and MEA under ambient pressure and an Arrhenius-type equation was established for the constant over temperature range from 25 °C to 45 °C. The corresponding activation energy was found to be 22.2 kJ/mol while the pre-exponential factor was equal to 1.09×10^9 L/(mol s). The equation is reliable and convenient to the design and simulation of CO_2 absorption process in microchannel.

1. Introduction

Global warming and climate change have motivated extensive researches towards developing improved and more efficient technologies for CO_2 capture from large point sources, such as natural gas, coal based power plant, floating liquefied natural gas plant (FLNG) and refinery off-gases. At present, the most widely utilized technique for CO_2 removal is CO_2 absorption by alkanolamine-based chemical solvents. Examples of the alkanolamines in gas treatment processes are monoethanolamine (MEA) [1–5], diethanolamine (DEA) [6], and activated methyldiethanolamine [7–10], etc.

Among the various alkanolamines, aqueous MEA is an important absorbent in CO_2 removal process and it has several advantages, such as high reactivity, low solvent cost, low molecular weight and thus high absorption capacity on a weight basis [11]. At present, industrial process of CO_2 absorption by aqueous MEA is usually conducted in column equipments with huge volume, but these equipments seem to be not suitable for CO_2 capture in some plants which need small absorption units, for example, in FLNG.

Microchannel reactor, compared with column equipments, possesses several advantages, such as small volume, huge surface to volume ratio, excellent mass and heat transfer abilities, and narrow residence time distribution, and hence can intensify some processes effectively, such as gas absorption [12,13], hydrogenation [14], nitration [15], and liquid–liquid two-phase extraction [16] etc.

Performance of microchannel reactor in gas absorption process was evaluated by TeGrotenhuis et al. [17]. They suggested that the microchannel technology could miniaturize chemical separation equipment by an order of magnitude, according to the result that over 90% of carbon dioxide was removed by DEA solution in less than 10 s from a stream containing 25% CO_2.

In addition, processes of pure CO_2 absorption into water, buffer solution and NaOH solution in microchannel were investigated systematically by Yue et al. [18]. The characteristics of liquid side mass transfer coefficient and interfacial area were studied

* Corresponding author. Tel.: +86 411 8437 9031; fax: +86 411 8437 9327.
E-mail address: gwchen@dicp.ac.cn (G. Chen).
URL: http://www.microchem.dicp.ac.cn (G. Chen).

1385-8947/$ - see front matter © 2013 Elsevier B.V. All rights reserved.
http://dx.doi.org/10.1016/j.cej.2013.03.053

Nomenclature

a	interfacial area, m^{-1}
a_S	specific surface area, m^{-1}
B	a base or bases
C	concentration, mol/L
d	depth of microchannel, mm
D_h	hydraulic diameter of microchannel, m
E_a	activation energy, kJ/mol
F	$\frac{1}{C_{CO_2,in}(2-\lambda)}\left[\ln\left\lvert\frac{X-1}{X-0.5\lambda}\right\rvert + \ln(0.5\lambda)\right]$, L/mol
k_1	reaction rate constant, $m^3/(mol\ s)$
k'_L	reaction rate constant for the reversible reaction of MEA with CO_2, L/(mol s)
k_B	reaction rate constant for the deprotonation of zwitterion by a base B, L/(mol s)
L	length of microchannel from T-junction to outlet, mm
m	reaction order of CO_2
MEA	monoethanolamine
λ	molar ratio of MEA to CO_2
n	reaction order of MEA
N	molar flow rate, mol s
P	pressure, MPa
Q	volumetric flow rate, mm/min
r	reaction rate between CO_2 and MEA, $mol/(m^3\ s)$
R_{CO_2}	absorption rate of CO_2 from gas phase to liquid phase, $mol/(m^2\ s)$
Re	Reynolds number
t	time, s
T	temperature, K
U	superficial velocity, m/s
V	volume of microchannel, m^3
w	width of microchannel, mm
X	CO_2 conversion
z	stoichiometric ratio of MEA to CO_2 in Eq. (5), $z = 1$

Greek letters

ρ	density, kg/m^3
μ	dynamic viscosity, Pa s

Subscripts

B	a base or bases
C	convection
D	diffusion
G	gas phase
in	T-junction of microchannel
L	liquid phase
MEA	monoethanolamine
N_2	nitrogen
out	outlet of microchannel

Superscripts

*	gas–liquid interface
$'$	homogeneous state

separately in different two-phase flow regimes, i.e., slug, slug-annular and churn flow, which demonstrated that both liquid side volumetric mass transfer coefficient and interfacial area in microchannel were at least one or two orders of magnitude higher than those in traditional gas–liquid contactors. What is more, the determined interfacial area between gas and liquid phases at annular flow pattern was approximately equal to the specific surface area of microchannel [18].

In a previous work [19], process characteristics of CO_2 absorption by MEA solution in a microchannel reactor were experimentally investigated and excellent results were obtained. After absorption, CO_2 concentration in gas phase could decrease directly from 32.3 vol.% to 300 ppm under certain conditions, which illustrates a promising prospect for CO_2 capture in microchannel reactor.

In this work, further investigation on the process of CO_2 absorption by MEA solutions in microchannel reactors was made and effects of relevant parameters were studied, i.e., MEA concentration, temperature, pressure, molar ratio of MEA to CO_2 (λ) and aspect ratio (ratio of depth to width of microchannel). The experiments were conducted with high gas flow rate, considering the requirements of industrial processes in which gas flow rate is usually very large. Meanwhile, a method was developed to determine the values of reaction rate constant for the reaction between CO_2 and MEA solution and an Arrhenius-type equation was proposed for the constant, depending on the process analysis on CO_2 absorption in microchannel reactors.

2. Experimental

2.1. Materials

Feed gas, a mixture of CO_2 and nitrogen (N_2), was purchased from Ke Na Science Technology Development Co., Ltd. The purities of both CO_2 and N_2 were 99%.

MEA with a purity of 99.5%, provided by Tianjin Guangfu Fine Chemical Research Institute, was used without further purification, while deionized water was boiled in order to remove the dissolved gases before utilization. MEA solutions were prepared from the MEA and the boiled deionized water by weight.

2.2. Apparatus and procedure

Experiments were conducted in three T-type, rectangular microchannels, which possessed a same width (w) of 0.7 mm but different depths (d) of 0.3, 0.5 and 0.7 mm. Besides, the lengths (L) of the microchannels from T-joint to outlet were all equal to 60 mm.

All microchannels were fabricated on smooth 316L stainless steel plates by precise machine, and then each of them was compressed against another smooth 316L stainless steel plate by screw fittings through the punched holes on the peripheries of both plates [20]. The thickness of all plates was 10 mm. Gas tightness of the formed microchannels was checked using N_2 under 2 MPa pressure.

As displayed in Fig. 1, the experimental setup, based on the previous work [19], mainly composed of a microchannel reactor, a gas–liquid separator, a mass flow controller, a constant-flow pump, a gas cylinder and a test section. The test section contained a soap film flowmeter and a CO_2 analyzer.

The reactor was placed in waterbath so as to maintain its temperature at a given value with an accuracy of ±0.1 K. Before entering into the reactor, both gas and liquid phases had to flow through two respective coiled stainless steel tubes, which were also placed in the waterbath, to be preheated to the given temperature. The outer diameter and thickness of the coils were 3 and 0.5 mm, respectively.

Feed gas was first regulated by a pressure reducing valve and then maintained by a mass flow controller (Beijing Sevenstar

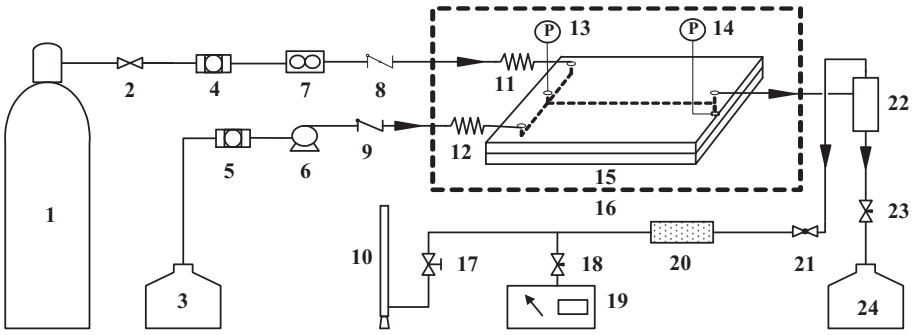

Fig. 1. Schematic of the experimental setup for CO_2 absorption in microchannel reactors. 1 – gas cylinder; 2 – pressure reducing valve; 3, 24 – liquid tank; 4, 5 – filter; 6 – constant-flow pump; 7 – mass flow controller; 8, 9 – check valve; 10 – soap film flowmeter; 11, 12 – coil; 13, 14 – pressure transducer; 15 – microchannel reactor; 16 – waterbath; 17 – Ball valve; 18, 23 – needle valve; 19 – CO_2 analyzer; 20 – silica gel drier; 21 – back pressure valve; 22 – gas–liquid separator.

Electronics Co., Ltd, measurement range: 0–1 L/min) at a given flow rate. When CO_2 absorption was conducted at pressures higher than 0.1 MPa, the back pressure valve would be used. The pressures at the T-junction and the outlet were measured by pressure transducers (Beijing Northking Electronic Technology Development Co., Ltd, CEMPX214). MEA solution was conveyed by a constant-flow pump (Series II, measurement range: 0–10 ml/min) before contacting the feed gas at the T-junction.

After flowing through the microchannel, the gas–liquid mixture was separated in the separator immediately, and then liquid phase flowed into the liquid tank, while gas phase flowed through a silica gel drier and then into the CO_2 analyzer (Ennix, FG10) or the soap film flowmeter. The silica gel drier had been swept by the feed gas for an hour before utilization and was used to remove a small quantity of the vapor of MEA solution so as to protect the CO_2 analyzer from contamination. When CO_2 concentration after absorption kept constant within 2 min, the value measured by the CO_2 analyzer would be recorded.

All experiments were repeated at least two times in order to guarantee the accuracy of the obtained results.

CO_2 conversion, X, based on CO_2 molar flow rates at the T-junction and the outlet, was used to evaluate the performance of MEA solutions,

$$X = (N_{CO_2,in} - N_{CO_2,out})/N_{CO_2,in} \times 100\% \quad (1)$$

where N denotes CO_2 molar flow rate. The equation is reasonable under the assumption, which was validated by experiments, that solubility of N_2 in MEA solutions is considered to be neglected.

The superficial velocities of gas and liquid phases were estimated using Eqs. (2) and (3), respectively, in which inlet volumetric flow rates of gas and liquid phases at ambient pressure and corresponding temperatures were used directly

$$U_G = Q_{G,in}/wd \quad (2)$$

$$U_L = Q_{L,in}/wd \quad (3)$$

where Q represents inlet volumetric flow rate and U is superficial velocity.

3. Results and discussion

3.1. Parametric analysis

3.1.1. Effects of aspect ratio

Aspect ratio of microchannel is one of the most important parameters in designing microchannel reactors and relates closely with the pressure drop along the microchannel as well as the performance of CO_2 absorbents. Its effects on CO_2 absorption process

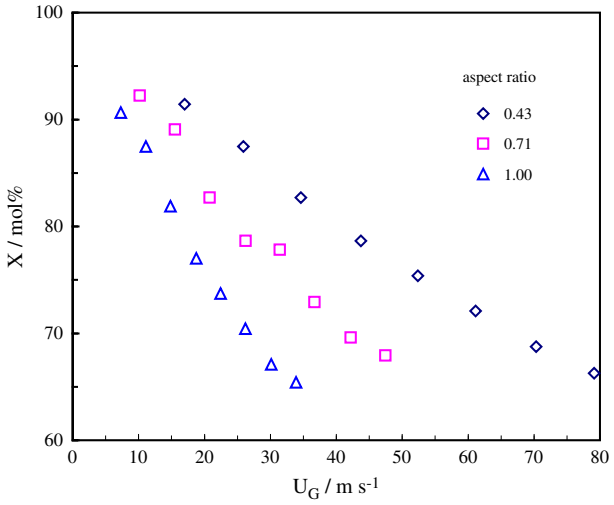

Fig. 2. Effects of aspect ratio on CO_2 conversion. T = 35 °C, P = 0.1 MPa, C_{CO_2} = 11.3 vol.%, C_{MEA} = 30 wt.%, λ = 2.27, U_G/U_L = 475.

was investigated utilizing microchannels with same width of 0.7 mm but different depths of 0.3, 0.5 and 0.7 mm. Values of the corresponding aspect ratio of microchannels were equal to 0.43, 0.71 and 1.0, respectively.

As demonstrated in Fig. 2, CO_2 conversion increases about 10% at the same gas phase superficial velocity when aspect ratio reduces from 1.0 to 0.43, because reduction in aspect ratio will result in smaller dimension of microchannel and higher reactant concentration gradient [21], which is beneficial for CO_2 mass transfer from gas phase to gas–liquid interface. In addition, the tendencies of CO_2 conversion along with gas phase superficial velocity become more smoothly as the aspect ratio reduces. This phenomenon can be attributed to that, at same gas phase superficial velocity, pressure drop gets larger as aspect ratio decreases. Since the pressures at the outlets of microchannels are all equal to 0.1 MPa, larger pressure drop means higher pressure along the microchannel, which can enhance the mass transfer driving force for CO_2 absorption. On the other hand, CO_2 conversion gradually decreases with increase in gas phase superficial velocity. For gas absorption in microchannel, two transport phenomena, i.e., diffusion and convection, compete with each other [22]. At 35 °C, diffusion coefficient of CO_2 in N_2, D_{CO_2} is found to be 0.18 cm^2/s [23], then diffusion times for CO_2 radial mass transfer towards gas–liquid interface estimated by Eqs. (4) and (5) were 2.5, 4.7 and 6.8 ms, respectively, in the microchannels with aspect ratio of 0.43, 0.71 and 1.0. While as gas phase superficial velocity increases, convection times for axial mass transfer

calculated by Eq. (6) reduce from 3.5 to 0.8 ms, from 5.8 to 1.3 ms and from 8.2 to 1.8 ms, respectively, in the above three microchannels. Consequently, at higher gas phase superficial velocity, the reduction in convection time can lead to insufficient diffusion time for CO_2 radial mass transfer from gas to liquid phase, which is detrimental for CO_2 conversion and can lead to the above tendencies

$$D_h = 2(w+d)/wd \tag{4}$$

$$t_D = (0.5D_h)^2/D_{CO_2} \tag{5}$$

$$t_C = L/U_G \tag{6}$$

3.1.2. Effects of MEA concentration

For CO_2 absorption at the same molar ratio of MEA to CO_2, flow rate of MEA solution can be diminished if higher concentration of MEA is utilized, which can save energy consumption at least for the transportation of the solution. Presently, MEA concentration in aqueous solution can go up to 25–30 wt.% with the addition of corrosion inhibitor [24].

As presented in Fig. 3, effects of MEA concentration were investigated using MEA solutions with concentrations of 10 wt.%, 20 wt.% and 30 wt.% and best absorption results were obtained by MEA solution with concentration of 30 wt.%, due to the differences in the reaction rate between CO_2 and MEA solutions, for higher CO_2 concentration could result in higher CO_2 absorption rate and thus stronger mass transfer enhancement by reaction.

3.1.3. Effects of temperature

As displayed in Fig. 4, effects of temperature were considered over the temperature range from 25 °C to 45 °C. Under the present conditions, temperature has positive effects on CO_2 conversion and CO_2 conversion can increase 5% when temperature rises from 25 °C to 35 °C or from 35 °C to 45 °C. On the one hand, mass transfer enhancement by reaction can be improved by the rise in temperature due to the increase in reaction rate constants; on the other hand, as the reaction temperature rises up, both diffusion coefficients of CO_2 and MEA in liquid phase increase, which is beneficial for CO_2 absorption, although CO_2 solubility in MEA solution declines [25].

3.1.4. Effects of pressure and molar ratio of MEA to CO_2

As shown in Fig. 5, compared with 0.1 MPa pressure, when CO_2 absorption operated under 1 MPa pressure, better results of CO_2 conversion were obtained and its tendencies along the gas flow rate were much more stable. For example, CO_2 conversion almost kept constant at 99.2% under 1 MPa pressure at the molar ratio of 3.72. At the same volumetric gas flow rate, convection time for CO_2 mass transfer at 1 MPa pressure is almost 10 times of that at 0.1 MPa pressure due to the compressibility of gas phase, besides, compressed gas phase contains more CO_2 per volume which is favorable for CO_2 solution into liquid phase and can result in stronger mass transfer driving force, as a result, more CO_2 will be consumed by reaction.

For the effects of molar ratio on CO_2 absorption, two values, i.e., 2.27 and 3.72, were studied both at 0.1 and 1 MPa pressure. From Fig. 5, we can see that higher molar ratio can result in higher CO_2 conversion, because more free MEA is present in liquid phase and can consume CO_2 more quickly, which can lead to faster CO_2 mass transfer rate from gas phase to liquid phase.

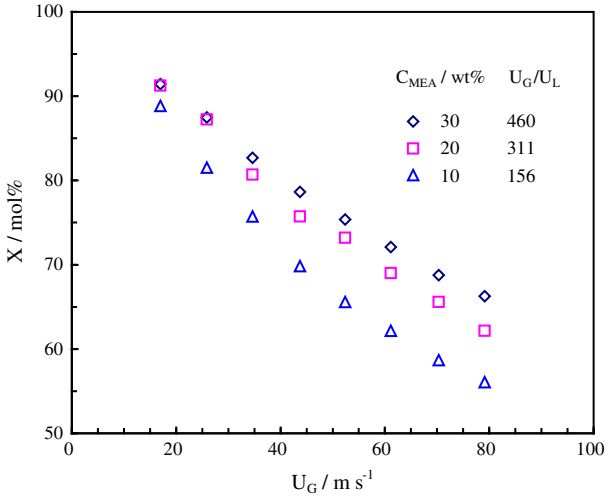

Fig. 3. Effects of concentration of MEA on CO_2 conversion. T = 25 °C, P = 0.1 MPa, C_{CO_2} = 11.3 vol.%, λ = 2.27, aspect ratio = 0.43.

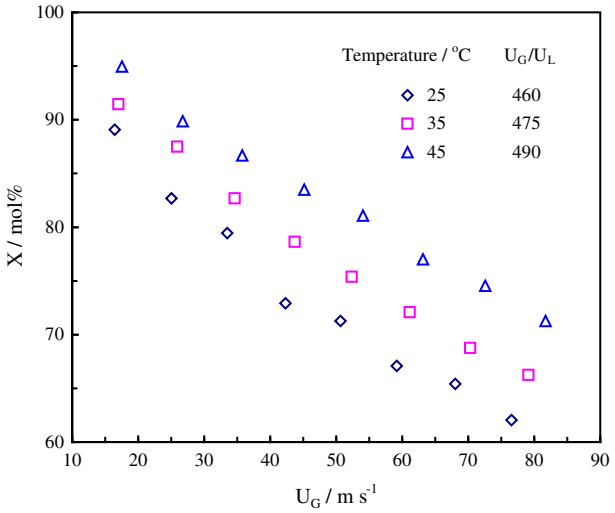

Fig. 4. Effects of temperature on CO_2 conversion. P = 0.1 MPa, C_{CO_2} = 11.3 vol.%, C_{MEA} = 30 wt.%, λ = 2.27, aspect ratio = 0.43.

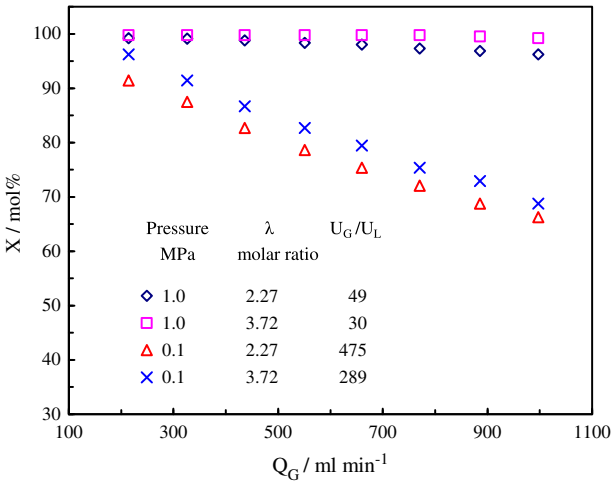

Fig. 5. Effects of pressure and molar ratio of MEA to CO_2 (λ) on CO_2 conversion. T = 35 °C, C_{CO_2} = 11.3 vol.% (0.1 MPa), 10.3 vol.% (1.0 MPa), C_{MEA} = 30 wt.%, aspect ratio = 0.43.

3.2. Reaction rate constant

Reaction rate constant is a parameter of critical importance to the design and simulation of CO_2 chemical absorption process. Techniques, such as laminar jet absorber, wetted wall column,

and stirred cell, have been used in deciding the constant with specified interfacial area and absence of interfacial waviness [26]. In most cases, CO_2 absorption rate is independent of contact time [27] and reaction rate constant is deduced from penetration theory under the assumption of pseudo-first order reaction [28].

In this work, however, it is difficult to derive the constant for CO_2 absorption in microchannel from penetration theory with the assumption of pseudo-first order reaction as mentioned above. The reasons will be analyzed in two respects, i.e., flow pattern and absorption rate, based on CO_2 absorption results in Fig. 4.

3.2.1. Flow pattern analysis

In Fig. 4, gas phase superficial velocity at the inlet is higher than 16 m/s, but liquid phase superficial velocity does not exceed 0.3 m/s, which demonstrates that the obtained experimental results are mainly located in the region of annular flow pattern, of which gas phase superficial velocity is usually larger than 10 m/s but liquid phase superficial velocity is less than 1 m/s [18]. This speculation can be confirmed by Fig. 6, in which annular flow patterns are obtained using high-speed CCD camera in microchannel with width of 0.7 mm and depth of 0.3 mm. Material of the microchannel is polymethyl methacrylate and details of the measurement of two-phase flow pattern can be seen in the work of Yue et al. [29]. The darkness presented in Fig. 6a and b is mainly resulted from the light refraction on the interface at the corners of the microchannel.

As shown in Fig. 6, as gas phase superficial velocity increases, liquid film becomes thinner for that shear force imposed on the gas–liquid interface by gas flow can be improved by the rise in gas phase superficial velocity. Moreover, the annular flow patterns always accompany with interfacial waviness at the gas phase superficial velocities of 27.8 m/s or 83.3 m/s. The waviness can change the crossing area that gas phase passes by and induce instabilities to the gas flow, which may cause the transition from laminar to turbulent flow at a smaller gas phase Reynolds number [30,31]. The gas phase Reynolds number in Fig. 6 ranges from 450 to 2200, which implies that some results are obtained with the presence of turbulence of gas phase. Reynolds number was estimated from Eq. (7) with density and dynamic viscosity of N_2 [32], since CO_2 concentration in gas phase did not exceed 11.3 vol.% and decreased along the microchannel

$$Re_G = \rho_{N_2} U_G D_h / \mu_{N_2} \tag{7}$$

3.2.2. CO_2 Absorption rate

CO_2 absorption rate is calculated using Eq. (8), assuming that the interfacial area, a, is equal to the specific surface area, a_S, of microchannel, as described in Eq. (9). In fact, the contact area aV between gas and liquid phases in annular flow pattern approximately equals to the internal surface area, $a_S V$, of microchannel [18], because the thickness of the liquid film is very small, compared with the dimension of microchannel [33]

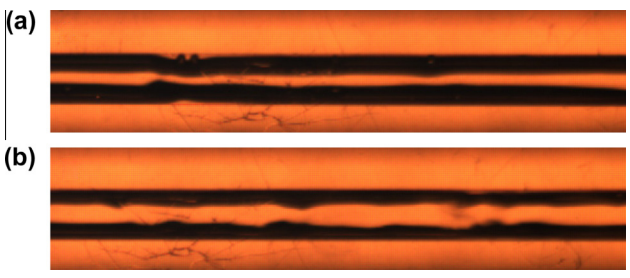

Fig. 6. Anuular flow patterns in the microchannel with aspect ratio of 0.43 using N_2 and water as agents: (a) U_G = 27.8 m/s, U_L = 0.3 m/s; and (b) U_G = 83.3 m/s, U_L = 0.3 m/s.

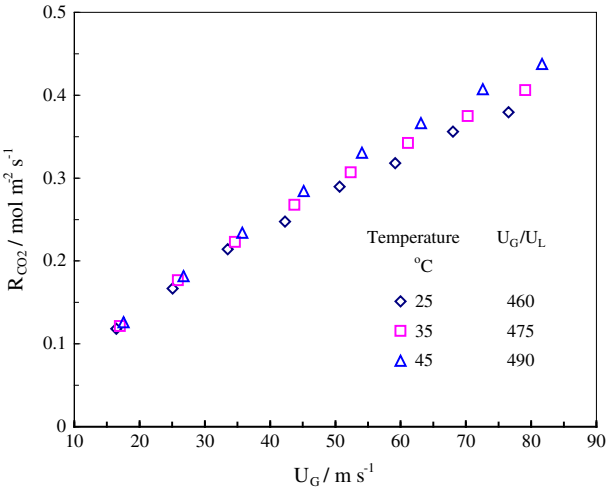

Fig. 7. CO_2 absorption rate for CO_2 absorption in microchannel in Fig. 4. P = 0.1 MPa, C_{CO_2} = 11.3 vol.%, C_{MEA} = 30 wt.%, λ = 2.27, aspect ratio = 0.43.

$$R_{CO_2} = (N_{CO_2,in} - N_{CO_2,out})/(aV) \tag{8}$$

$$aV = a_S V = 2(w + d)L \tag{9}$$

As presented in Fig. 7, CO_2 absorption rate in Fig. 4 varies from 0.1 to 0.45 mol/(m^2 s) and ascends both with temperature and gas phase superficial velocity.

As temperature goes up, mass transfer enhancement by reaction can be promoted, besides, diffusion of CO_2 and MEA in liquid phase can become more easily due to the reduction of viscosity in MEA solution, which can contribute to the positive effects of temperature on CO_2 absorption rate.

When CO_2 absorption process is conducted at higher gas phase superficial velocity, more CO_2 will flow through the microchannel, besides, mass transfer resistance for CO_2 transfer from gas to liquid phases will be reduced, as a result, more CO_2 will be absorbed by MEA solution. However, this tendency is different with that in laminar jet absorber [26] and wetted wall column [27], in which CO_2 absorption rate is almost independent of gas–liquid contact time and a constant value of CO_2 absorption rate is gained at given temperature. Consequently, for a given temperature in laminar jet absorber or wetted wall column, only one value of reaction rate constant can be deduced from penetration theory under the assumption of pseudo-first order reaction at various gas–liquid contact times. But for CO_2 absorption in microchannel, values of the reaction rate constant cannot be consistent at different gas–liquid contact times, if we use the same method as that in laminar jet absorber or wetted wall column.

3.2.3. Determination of reaction rate constant

Based on the above analysis, it is necessary to propose a method to determine the reaction rate constant between CO_2 and MEA solution in microchannel, due to the presence of interfacial waviness as well as the trend of CO_2 absorption rate along with the gas phase superficial velocity. Prior to develop the method, reaction kinetics between CO_2 and MEA solution should be analyzed in detail.

3.2.3.1. Kinetic analysis. Due to its primary amine characteristics, when MEA absorbs CO_2, the reaction of carbamate formation takes place:

$$CO_2 + 2MEA \leftrightarrow MEACOO^- + MEAH^+ \tag{10}$$

According to the zwitterion mechanism proposed by Caplow [34] and reintroduced by Danckwerts [35], the reaction usually involves the formation of zwitterion:

$$CO_2 + MEA \overset{k_1}{\underset{k_{-1}}{\leftrightarrow}} MEAH^+COO^- \quad (11)$$

and the subsequent deprotonation of the zwitterion by a base or bases B:

$$MEAH^+COO^- + B \overset{k_B}{\rightarrow} MEACOO^- + BH^+ \quad (12)$$

where B can be species MEA, OH^-, CO_3^{2-}, HCO_3^- or H_2O. In our experiments, CO_2 loading, i.e., mole of CO_2/mole of MEA, was not more than 0.45 after absorption, under this condition, the main products in the loaded solution are $MEAH^+$ and $MEACOO^-$ and the concentrations of OH^-, CO_3^{2-}, HCO_3^- and, especially, free CO_2 are very low [26]. Therefore, the main contribution to the deprotonation of the zwitterion comes from MEA, and to a less extent from OH^-, CO_3^{2-}, HCO_3^- or H_2O, since the deprotonation ability of a base mainly depends on its concentration as well as how strong a base is [36].

With steady-state principle to the intermediate zwitterions, the rate of reaction of CO_2 with MEA solutions can be expressed as:

$$r = \frac{k_1 C_{CO_2} C_{MEA}}{1 + \frac{k_1}{k_B C_B}} \quad (13)$$

For MEA, deprotonation of the zwitterions is almost instantaneous as compared to the reverse reaction in Eq. (11) [26], that is,

$$k_{-1} \ll k_B C_B \quad (14)$$

and hence Eq. (13) can be transformed to:

$$r = k_1 C_{CO_2} C_{MEA} \quad (15)$$

3.2.3.2. Method of determination. A method is developed to determine the apparent values of reaction rate constant k_1 in Eq. (15) at various temperatures, taking into account the process characteristics of CO_2 absorption in microchannel. As shown in Fig. 4, CO_2 conversion decreases linearly, to some extent, with the rise in gas phase superficial velocity, in addition, gas phase is continuous through the microchannel, as illustrated in Fig. 6.

The method is based on the assumption that reaction between CO_2 and MEA is considered to be a homogeneous gas phase reaction. With this treatment, only one value of k_1 will be obtained at a given temperature from CO_2 conversion at different gas phase superficial velocities in Fig. 4.

Under this assumption, Eq. (15) can be rewritten as Eq. (16), in which C'_{MEA} is the concentration of MEA at the homogeneous state

$$r = k_1 C_{CO_2} C'_{MEA} \quad (16)$$

According to the definition of molar ratio of MEA to CO_2 (λ), the quotient between the concentrations of MEA and CO_2 at the homogeneous state should be equal to λ, as described in the following equation

$$C'_{MEA,in} / C_{CO_{2,in}} = \lambda \quad (17)$$

As shown in Eq. (10), two moles of MEA will be consumed by one mole of CO_2 in the absorption process. Then Eq. (16) can be transformed into

$$r = -dC_{CO_2}/dt = k_1 C_{CO_2} C'_{MEA}$$
$$= k_1 C_{CO_2,in}(1 - X)(C'_{MEA,in} - 2XC_{CO_2,in}) \quad (18)$$

Eq. (18) can be simplified and written as follows:

$$\frac{dX}{(1 - X)(0.5\lambda - X)} = 2C_{CO_2,in} k_1 dt \quad (19)$$

At a given temperature, gas–liquid contact time t_C is corresponded to CO_2 conversion X in Fig. 4. The contact time t_C is calculated using Eq. (6). And it is easy to understand that when t_C is 0, CO_2 conversion X should also be equal to 0. By integration with contact time and CO_2 conversion, Eq. (21) can be deduced from the following equation

$$\int_0^X \frac{dX}{(1 - X)(0.5\lambda - X)} = 2C_{CO_2,in} \int_0^{t_C} k_1 dt \quad (20)$$

$$F = \frac{1}{C_{CO_2,in}(2 - \lambda)} \left[\ln \left| \frac{X - 1}{X - 0.5\lambda} \right| + \ln(0.5\lambda) \right] = k_1 t_C \quad (21)$$

Finally the value of reaction rate constant k_1 can be acquired from the slope of the plot of F vs. t_C, as displayed in Fig. 8. As demonstrated by Eqs. (22)–(27), excellent linear relationship is found to exist between F and t_C at temperatures of 25 °C, 35 °C and 45 °C

$$F_{25} = 141346 t_C \quad (22)$$

$$R^2_{25} = 0.9748 \quad (23)$$

$$F_{35} = 180950 t_C \quad (24)$$

$$R^2_{35} = 0.9773 \quad (25)$$

$$F_{45} = 248946 t_C \quad (26)$$

$$R^2_{45} = 0.9936 \quad (27)$$

Values of the reaction rate constant obtained from Eqs. (22)–(27) are 141346, 180950 and 248946 L/(mol s), respectively, at temperatures of 25 °C, 35 °C and 45 °C. An Arrhenius-type equation, Eq. (28), is proposed for the reaction rate constant, based on the linear relationship between $\ln k_1$ and $1/T$, as revealed in Fig. 9. The corresponding activation energy is found to be 22.2 kJ/mol and the pre-exponential factor is equal to 1.09×10^9 L/(mol s)

$$k_1 = 1.09 \times 10^9 \exp(-2671.4/T) \quad (28)$$

$$E_a = 22.2 \ \text{kJ/mol} \quad (29)$$

The apparent values of reaction rate constant determined for CO_2 absorption by MEA solution in microchannel are larger than those in laminar jet absorber [26] and wetted wall column [37]. In laminar jet absorber [26], values of the reaction rate constant range from 5338 to 27,706 L/(mol s), while in wetted wall column [37], values of the reaction rate constant are in the scope from 4446 to 13,813 L/(mol s).

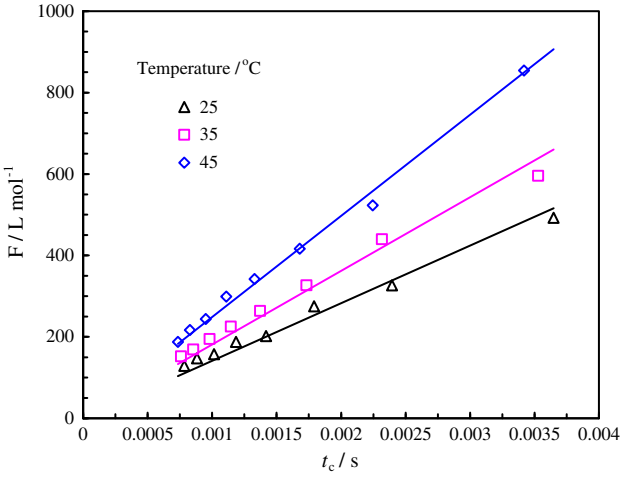

Fig. 8. Relationship between F vs. t_C at temperatures of 25 °C, 35 °C and 45 °C.

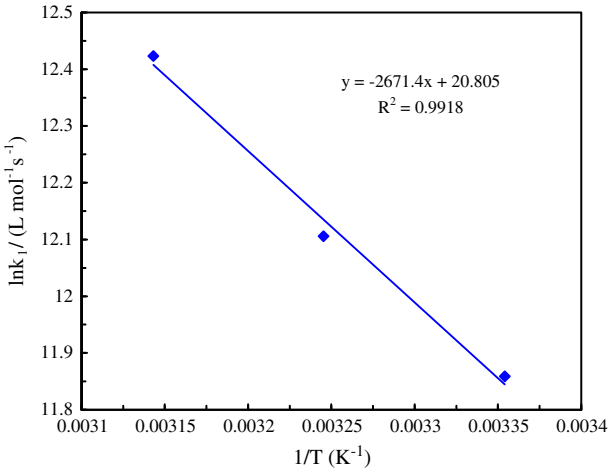

Fig. 9. Relationship between the apparent second-order rate constant k_1 and temperature.

Compared with laminar jet absorber and wetted wall column, higher reactant concentration gradient can be achieved in microchannel with smaller dimension [21] and thus it needs less diffusion time for CO_2 transfer from gas phase to gas–liquid interface. As mention above, interfacial waviness is always present on the gas–liquid interface. On the one hand, the waviness has an influence on the characteristics of gas flow and is favorable for the mixing of CO_2 in gas phase; on the other hand, the waviness can promote the surface renewal process on the interface and can transport CO_2 from the interface to liquid phase effectively. All these factors can improve the process CO_2 absorption in microchannel and lead to a higher CO_2 absorption rate, which is beneficial for CO_2 reaction with MEA solution and can result in a bigger apparent reaction rate constant.

4. Conclusions

Process of CO_2 absorption by MEA solutions has been investigated in microchannel reactors and effects of several parameters on the process have been analyzed. Depending on the experimental results, CO_2 absorption will yield better results if experiments are conducted at higher temperature, pressure and concentration of MEA in microchannel with smaller aspect ratio.

Due to the presence of interfacial waviness as well as the tendency of CO_2 absorption rate along with gas phase superficial velocity, it is not feasible to deduce reaction rate constant from penetration theory under the assumption of pseudo-first order reaction.

Considering the process characteristics of CO_2 absorption in microchannel, a method is developed to determine the values of reaction rate constant between CO_2 and MEA under ambient pressure and an Arrhenius-type equation is proposed for the reaction rate constant, which can offer convenience for the design and simulation of CO_2 absorption process in microchannels.

Acknowledgements

We acknowledge gratefully the financial supports for this project from National Natural Science Foundation of China (No. 21225627), Strategic Priority Research Program of the Chinese Academy of Sciences (No. XDA07040103) and Ministry of Science and Technology of China (No. 2009CB219903).

References

[1] K.K. Akanksha, V.K. Pant, Srivastava, mass transport correlation for CO_2 absorption in aqueous monoethanolamine in a continuous film contactor, Chem. Eng. Proc. 47 (2008) 920–928.
[2] J.M. Plaza, D.V. Wagener, G.T. Rochelle, Modeling CO_2 capture with aqueous monoethanolamine, Int. J. Greenhouse Gas Control 4 (2010) 161–166.
[3] G. Puxty, R. Rowland, M. Attalla, Comparison of the rate of CO_2 absorption into aqueous ammonia and monoethanolamine, Chem. Eng. Sci. 65 (2010) 915–922.
[4] S. Freguia, G.T. Rochelle, Modeling of CO_2 capture by aqueous monoethanolamine, AIChE J. 49 (2003) 1676–1686.
[5] J.H. Meldon, M.A. Morales-Cabrera, Analysis of carbon dioxide absorption in and stripping from aqueous monoethanolamine, Chem. Eng. J. 171 (2011) 753–759.
[6] H. Hikita, S. Asai, H. Ishikawa, K. Uku, Absorption of carbon-dioxide into aqueous diethanolamine solutions, Chem. Eng. Commun. 5 (1980) 315–322.
[7] S. Bishnoi, G.T. Rochelle, Absorption of carbon dioxide in aqueous piperazine/methyldiethanolamine, AIChE J. 48 (2002) 2788–2799.
[8] A.B. Rao, E.S. Rubin, A technical, economic, and environmental assessment of amine-based CO_2 capture technology for power plant greenhouse gas control, Environ. Sci. Technol. 36 (2002) 4467–4475.
[9] T. Sema, A. Naami, K. Fu, M. Eadli, H. Liu, H. Shi, Z. Liang, R. Idem, P. Tontiwachwuthikul, Comprehensive mass transfer and reaction kinetics studies of CO_2 absorption into aqueous solutions of blended MDEA–MEA, Chem. Eng. J. 209 (2012) 501–512.
[10] A. Samanta, S.S. Bandyopadhyay, Absorption of carbon dioxide into piperazine activated aqueous N-methyldiethanolamine, Chem. Eng. J. 171 (2011) 734–741.
[11] N. McCann, M. Maeder, M. Attalla, Simulation of enthalpy and capacity of CO_2 absorption by aqueous amine systems, Ind. Eng. Chem. Res. 47 (2008) 2002–2009.
[12] J.D. Martin, S.D. Hudson, Mass transfer and interfacial properties in two-phase microchannel flows, New. J. Phys. 11 (2008) 1–26.
[13] J. Yue, R. Boichot, L. Luo, Y. Gonthier, G.W. Chen, Q. Yuan, Flow distribution and mass transfer in a parallel microchannel contactor integrated with constructal distributors, AIChE J. 56 (2010) 298–317.
[14] J. Kobayashi, Y. Mori, S. Kobayashi, Hydrogenation reactions using $scCO_2$ as a solvent in microchannel reactors, Chem. Commun. 20 (2005) 2567–2568.
[15] J.N. Shen, Y.C. Zhao, G.W. Chen, Q. Yuan, Investigation of nitration processes of iso-octanol with mixed acid in a microreactor, Chin. J. Chem. Eng. 17 (2009) 412–418.
[16] Y.H. Su, G.W. Chen, Y.C. Zhao, Q. Yuan, Intensification of liquid-liquid two-phase mass transfer by gas agitation in a microchannel, AIChE J. 55 (2009) 1948–1958.
[17] W.E. TeGrotenhuis, R.J. Cameron, V.V. Viswanathan, R.S. Wegeng, Solvent extraction and gas absorption using microchannel contactors, in: 3rd International Conference on Microreaction, Technology, 2000, pp. 541–549.
[18] J. Yue, G.W. Chen, Q. Yuan, L. Luo, Y. Gonthier, Hydrodynamics and mass transfer characteristics in gas-liquid flow through a rectangular microchannel, Chem. Eng. Sci. 62 (2007) 2096–2108.
[19] C.B. Ye, G.W. Chen, Q. Yuan, Process Characteristics of CO_2 absorption by aqueous monoethanola mine in a microchannel reactor, Chin. J. Chem. Eng. 20 (2012) 111–119.
[20] J. Yue, L. Luo, Y. Gonthier, G.W. Chen, Q. Yuan, An experimental study of air-water Taylor flow and mass transfer inside square microchannels, Chem. Eng. Sci. 64 (2009) 3697–3708.
[21] H. Lowe, W. Ehrfeld, State-of-the-art in microreaction technology: concepts, manufacturing and applications, Electrochim. Acta. 44 (1999) 3679–3689.
[22] H. Monnier, L. Falk, Intensification of G/L absorption in microstructured falling film. Application to the treatment of chlorinated VOC's – Part II: modeling and geometric optimization, Chem. Eng. Sci. 66 (2011) 2475–2490.
[23] W.J. Massman, A review of the molecular diffusivities of H_2O, CO_2, CH_4, CO, O_3, SO_2, NH_3, N_2O, NO, and NO_2 in air, O_2 and N_2 near STP, Atmos. Environ. 32 (1998) 1111–1127.
[24] F.H. Al-Masabi, M. Castier, Simulation of carbon dioxide recovery from flue gases in aqueous 2-amino-2-methyl-1-propanol solutions, Int. J. Greenhouse Gas Control 5 (2011) 1478–1488.
[25] G.F. Versteeg, W.V. Swaalj, Solubility and diffusivity of acid gases (CO_2, N_2O) in aqueous alkanolamine solutions, J. Chem. Eng. Data. 33 (1988) 29–34.
[26] A. Aboudheir, P. Tontiwachwuthikul, A. Chakma, R. Idem, Kinetics of the reactive absorption of carbon dioxide in high CO_2-loaded, concentrated aqueous monoethanolamine solutions, Chem. Eng. Sci. 58 (2003) 5195–5210.
[27] A.K. Saha, S.S. Bandyopadhyay, A.K. Biswas, Kinetics of absorption of CO_2 into aqueous-solutions of 2-amino-2-methyl-1-propanol, Chem. Eng. Sci. 50 (1995) 3587–3598.
[28] R.J. Littel, G.F. Versteeg, W.P.M. Vanswaaij, Kinetics of CO_2 with primary and secondary-amines in aqueous-solutions. 2. Influence of temperature on zwitterion formation and deprotonation rates, Chem. Eng. Sci. 47 (1992) 2037–2045.
[29] J. Yue, L. Luo, Y. Gonthier, G.W. Chen, Q. Yuan, An experimental investigation of gas-liquid two-phase flow in single microchannel contactors, Chem. Eng. Sci. 63 (2008) 4189–4202.

[30] G.L. Morini, M. Lorenzini, S. Salvigni, M. Spiga, Analysis of laminar-to-turbulent transition for isothermal gas flows in microchannels, Microfluid. Nanofluid. 7 (2009) 181–190.
[31] P.Y. Wu, W.A. Little, Measurement of friction factors for the flow of gases in very fine channels used for microminiature joule-thomson refrigerators, Cryogenics 23 (1983) 273–277.
[32] D. Seibt, E. Vogel, E. Bich, D. Buttig, E. Hassel, Viscosity measurements on nitrogen, J. Chem. Eng. Data. 51 (2006) 526–533.
[33] M. Roudet, K. Loubiere, C. Gourdon, M. Cabassud, Hydrodynamic and mass transfer in inertial gas-liquid flow regimes through straight and meandering millimetric square channels, Chem. Eng. Sci. 66 (2011) 2974–2990.
[34] M. Caplow, Kinetics of carbamate formation and breakdown, J. Amer. Chem. Soc. 90 (1968) 6795–6803.
[35] P.V. Danckwerts, Reaction of CO_2 with ethanolamines, Chem. Eng. Sci. 34 (1979) 443–446.
[36] B.P. Mandala, A.K. Biswas, S.S. Bandyopadhyay, Absorption of carbon dioxide into aqueous blends of 2-amino-2-methyl-1-propanol and diethanolamine, Chem. Eng. Sci. 58 (2003) 4137–4144.
[37] S.Y. Horng, M.H. Li, Kinetics of absorption of carbon dioxide into aqueous solutions of monoethanolamine plus triethanolamine, Ind. Eng. Chem. Res. 41 (2002) 257–266.